Electrical conductivity of a strongly coupled plasma

I. T. Yakubov

IVTAN Scientific Combine of the Russian Academy of Sciences, Moscow
(Submitted 3 June 1992; resubmitted 29 December 1992)
Usp. Fiz. Nauk **163**, 35–51 (May 1993)

The electrical conductivity is examined throughout the entire range of strongly coupled states of matter: in gases, liquids, and strongly ionized high-density plasmas. These states are classified and the phase diagram is broken up into regions, depending on the nature of the strongly coupled behavior and its occurrence. After a brief discussion of the electrical conductivity of an ideal plasma, the clearest and most thoroughly developed theoretical models are presented. The available experimental data are described and compared with theory. The variations in the electrical conductivity with density and temperature over many orders of magnitude are described.

1. INTRODUCTION

The electrical conductivity is the most indicative and easily observed property of a plasma. It determines the dissipative heating of the plasma and its interaction with an external field. The strongly coupled plasma states described below occupy a region in the phase diagram that extends over gaseous, liquid, and specifically plasma materials, i.e., heated states. In this space, specified in terms of temperature (from normal to atomic) and density (from very low-density plasma to highly compressed liquid), the electron states, i.e., the ionization level and its mobility change drastically. The electrical conductivity is very sensitive to the electron state. In the transition of a metal from a liquid to a weakly conducting gas phase it varies from a state of almost free electrons in a liquid metal to electrons strongly bound to atoms. Then the electrical conductivity varies by many orders of magnitude. The problem is to describe it under conditions such that the volume of existing experimental data is still very restricted.

Only in a low-density plasma and in a liquid metal near the melting point can the electrons be regarded as free or almost free, so that we can we use the results of gas kinetic theory. Throughout most of the phase space we are dealing with highly correlated systems due to the significant interparticle interaction. The latter can take various forms—Coulombic, polarization, and more complicated—and manifests itself differently in regions as partial or multiple ionization. We should not suppose that a single prescriptive theory can be derived here. However, models can be proposed of the phenomena which are largely based on ideas in related areas of physics, and also on the experimental data.

This review summarizes the results of investigations carried out in the last decade, which enable us to present a picture of the variation in the electrical conductivity over the whole range of parameters. The review is constructed as follows.

We start by giving a classification of the states of strong coupled plasmas. The "density–temperature" phase diagram is broken up into regions depending on the behavior of the interparticle interaction and how it arises. Next we briefly discuss the electrical conductivity of an ideal plasma. Then we arrive at the main material of the present review, in which we treat the physically clearest and at the same time most prescriptive theoretical approaches describing electrical conductivity in the various regions. The agreement between the calculated values of the electrical conductivity and the experimental results is discussed. In the last section some results are presented from calculations of the electrical conductivity over a broad range of parameters necessary for solving applied problems. The thermal emf is briefly considered in an appendix; this is closely related to the electrical conductivity.

In this review we restrict ourselves to the time-independent electrical conductivity. Reference are given only to the work directly used in this review.

2. DEFINITION OF STRONGLY COUPLED PLASMA AND CLASSIFICATION OF STATES

A material is strongly coupled if the average interparticle interaction energy is comparable with or greater than the average kinetic energy of the interacting particles. The ratio of these two energies yields the criterion for strong coupling. In a plasma made up of ions of charge Z (more precisely, Z is the charge state) and electrons there are three kinds of interaction: ion–ion, ion–electron, and electron–electron. Correspondingly there are three strong coupling parameters. If the electrons are not degenerate then

$$\Gamma_{ZZ}=Z^2e^2/\bar{r}T, \quad \Gamma_{Ze}=Ze^2/\bar{r}T,$$
$$\Gamma_{ee}=Z^{1/3}e^2/\bar{r}T; \tag{1}$$

here $\bar{r}=(4\pi N_i/3)^{-1/3}$ is the average separation between ions, which under strong-coupling conditions plays the role of a shielding length; the quantity $\bar{r}$ is $Z^{1/3}$ times larger than the interelectron separation $r_s=(4\pi N_e/3)-^{1/3}$; N_e and N_i are the electron and ion densities, $ZN_i=N_e$.

In weakly coupled plasmas the charges are shielded from one another at distances of order the Debye radius r_D rather than at the interparticle separation as in the limit

 1063-7869/93/050365-15$10.00

$\Gamma_{Ze} \gg 1$. Weak coupling is consequently measured in terms of the Debye coupling parameter. If the plasma is nondegenerate,

$$\Gamma_D = Ze^2/r_D T, \quad r_D = (4\pi e^2 N_e/T)^{-1/2}.$$

It is equal to the ratio of the Coulomb interaction energy calculated in the self-consistent field approximation to the thermal energy. However, since $\Gamma_{Ze} \sim \Gamma_D^{2/3}$ holds, both of these (the Madelung and Debye parameters) are equivalent.

If the Fermi energy $E_F = (3\pi e^2 N_e)^{2/3}\hbar/2m$ exceeds the temperature, the electron subsystem is degenerate. Then

$$\Gamma_{ZZ} = Z^2 e^2/\bar{r}T, \quad \Gamma_{Ze} = Z^{2/3} r_s/a_0, \quad \Gamma_{ee} = r_s/a_0. \qquad (2)$$

Note that if we replace T with E in Eq. (1) for Γ then we have $\Gamma_{ee} = 2r_s/a_0$. In the literature, however, it is customary to take $\Gamma_{ee} = r_s/a_0$.

It turns out to be important that at large values $Z \gg 1$ of the ion charge we have the inequalities

$$\Gamma_{ZZ} \gg \Gamma_{Ze} \gg \Gamma_{ee}. \qquad (3)$$

These conditions are conducive to theoretical analysis, since they enable us to concentrate mainly on the ion–ion interaction, which can be very large, $\Gamma_{ZZ} \gg 1$ and treat the electron–ion interaction approximately, $\Gamma_{Ze} \approx 1$, while the electron–electron interaction is found to be weak, $\Gamma_{ee} \ll 1$. These conditions hold, e.g., in the experiments of Kormer (see, e.g., Ref. 1). Specimens of porous copper were compressed by powerful shock waves. This permitted high energy densities to be achieved with copper densities close to 10 g/cm^3 and a temperature of 20 eV. It was found that $\Gamma_{ZZ} = 11$, $\Gamma_{Ze} = 2$, $\Gamma_{ee} = 0.6$.

A strongly coupled singly ionized plasma is the most complicated object for theory, since for $Z = 1$ all three coupling parameters are the same. Consequently, for $\Gamma > 1$ all three Coulomb interactions become equally strong. However, this region has already been studied in a considerable number of laboratories. The available experimental data can be employed to derive a dimensionless Coulomb electrical conductivity which is a universal property of the Coulomb plasma.

At low temperatures and densities the Coulomb interaction results in the formation of bound states, i.e., atoms and complex ions. The former are described by the Saha equations. For $I > T$ the plasma is partially ionized, where I is the ionization potential of the atom. Cold ionization results from strong compression. The ion radius R_i depends on its charge Z and the nuclear charge Z_n, $R_i = R_i(Z_n, Z)$. It cannot be larger than the average interparticle separation. Setting them equal yields an equation for the value of the charge Z that occurs in compressed material:

$$R_i(Z_n, Z) = \bar{r}.$$

The Coulomb interaction is not the only type of interaction possible. The interaction between a complex ion and an electron at distances comparable with the ion radius is enhanced, since the nucleus is not completely screened by the bound electrons. The ion radius is equal to the Thomas–Fermi radius in order of magnitude, $R_i \sim a_0(Z_n - Z)^{1/3}$, where Z_n is the charged state of the nucleus.

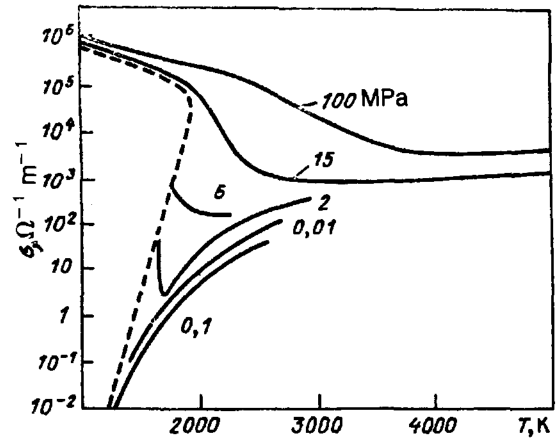

FIG. 1. Isobars of the electrical conductivity of cesium, obtained by various authors (see bibliography in Ref. 1). The broken curve is the electrical conductivity on the gas–liquid transition line.

In a weakly ionized plasma the interactions between charges and neutral atoms and molecules is significant. The polarization forces are the most important. The total potential produced at the location of the ion by the atoms surrounding it, divided by the temperature, serves as the coupling parameter:

$$\Gamma_{ai} = 2\pi\alpha e^2 N_a/R_a T; \qquad (4)$$

here α is the atomic polarizability and R_a is the atomic radius. The quantities R_a are of order e^2/I, where I is the atomic ionization energy. While it is naturally weaker than the Coulomb interaction, this interaction can also form bound states. In metal vapors the occurrence of molecular and cluster ions, which shift the ionization equilibrium, changes the electrical conductivity.

Consider the way in which the interparticle interactions are manifested in the magnitudes of the electrical conductivity for the case of cesium. Figure 1 was plotted from the results of a large number of experimental and theoretical treatments. Shown are the curves of constant electrical conductivity on the gas–liquid transition curve. In Fig. 2 the density–temperature plane is divided up into a number of characteristic regions.

In the vapor phase (region *VI*) the electrical conductivity increases with heating due to thermal ionization and as a function of pressure decreases in proportion to $p^{-1/2}$, which agrees with the formulas of gas kinetics. But in dense vapor these simple formulas become more complicated. Near the 1-atm (or 10-atm) isobar the strong coupling causes the sign of $(d\sigma/dp)_T$ to change, and the isobars become nonmonotonic. These effects (region *IV*) are due to the interaction of the ions and electrons with atoms and to the formation of cluster ions.

In liquid the electrical conductivity decreases in response to heating and increases as a function of pressure. The decrease in conductivity associated with heating is particularly abrupt on isobars with pressures close to the

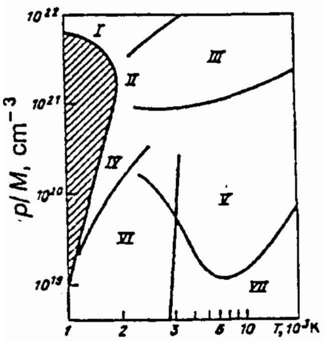

FIG. 2. Phase diagram in $\rho - T$ space for cesium.[2] The regions are labeled according to *I*) liquid metal, *II*) metal–insulator transition, *III*) strongly coupled completely ionized plasma, *IV*) strongly coupled metal–vapor plasma (weakly ionized plasma), *V*) weakly coupled strongly ionized plasma, *VI*) weakly coupled plasma of metal vapor, *VII*) ideal highly ionized plasma.

critical value. Here in region *II* the Mott metal–insulator transition occurs, since the electrons are bound in the atoms. The electrical conductivity passes through a minimum on the isobar. With further heating, which gives rise to an increase in the degree of ionization, the isobars of σ pass to the region of strong coupling in a highly ionized plasma, region *III*. Sooner or later at high temperatures all the isobars go over to their Spitzer values, corresponding to an ionized plasma with intermediate values of the coupling. These values depend only logarithmically on the pressure. Consequently, in Fig. 1 all the isobars gradually converge.

Material densities corresponding to number densities of 10^{22} particles per cm^3 and higher in cesium are attained when larger values of the pulsed energy are deposited in condensed material. This is the multiply ionized region, reached by high compression. The first experimental results have already been obtained in this interesting region.

3. ELECTRICAL CONDUCTIVITY OF A WEAKLY COUPLED PLASMA

In a weakly ionized plasma we can disregard the interaction with the ions and the electron–electron interaction, and include only the interactions of the electrons with the gas atoms (or molecules). If this gas can be treated as weakly coupled, and the interaction between the electron and its atoms can be regarded as independent two-particle collisions, then the Lorentz gas approximation is applicable.

For a nondegenerate plasma this approximation yields (see, e.g., Ref. 3)

$$\sigma = (4/3\sqrt{\pi}) e^2 N_e m^{-1} T^{-5/2} \int_0^\infty E^{3/2} \nu(E)^{-1} \times \exp(-E/T) \mathrm{d}E, \tag{5}$$

where $\nu(E) = N_a q(E)(2E/m)^{1/2}$ is the collision frequency, N_a is the atomic (molecular density), and $q(E)$ is the momentum-transfer cross section.

In a highly ionized plasma collisions with ions dominate. If the plasma is not degenerate, its electrical conductivity is given by the Spitzer formula

$$\sigma = \gamma_E(Z) \cdot 2(2T)^{3/2} (\pi^{3/2} Z e^2 m^{1/2} \ln \Lambda)^{-1},$$

$$\Lambda = \ln(3/\Gamma_D), \tag{6}$$

where Z is the charge number of the ion. The effect of the long-range Coulomb interaction consists of multiple scattering through small angles, taken into account by the Coulomb logarithm $\ln \Lambda$. The magnitude of Λ in a classical plasma is determined by the ratio of the maximum impact parameter (the screening length, i.e., the Debye length) to the minimum impact parameter, the Landau length. This ratio is the same as the plasma coupling parameter Γ_D.

At high temperatures, when the Landau length is smaller than the thermal wavelength of an electron, the latter assumes the role of the minimum impact parameter and goes into the expression for Λ.

The Spitzer factor $\gamma_E(Z)$ distinguishes Eq. (6) from that which would arise if we were to calculate the electrical conductivity of a strongly ionized plasma by using the Lorentz approximation (5). The factor $\gamma_E(Z)$ takes into account the role of electron–electron collisions. For charge state Z equal to 1, 2, 4, 16, and ∞ the factor $\gamma_E(Z)$ is equal to 0.582, 0.683, 0.785, 0.923, and 1.000, respectively. The electron–electron interactions reduce the electrical conductivity. The way this works is that in an external electrical field the electron distribution function is stretched out parallel to the field. The electron–electron interactions, which are opposed to this, only symmetrize the electron distribution and result in a decrease in the transport coefficients. In the high-Z limit the factor γ_E approaches unity, since the role of the electron–electron collisions is less important in comparison with that of electron–ion collisions.

Equation (6) is asymptotically exact in the limit $\ln \Lambda \gg 1$. A number of investigators have calculated the next terms in the σ expansion, i.e., the nonlogarithmic terms. These, however, do not significantly extend the region of applicability of Eq. (6).

If the temperature are high but the ions are not completely stripped, then the Coulomb scattering amplitude Ze^2/T becomes comparable with the characteristic radius R_i of a complex ion. Then non-Coulomb scattering from the ions becomes important.

The plasma may be regarded as strongly ionized if the electrons collide more often with the ions than with the atoms. Equating these collision frequencies we find

$$qN_a = (\pi e^4/T^2) N_e \ln \Lambda. \tag{7}$$

Equation (7) yields an equation for the curve which divides regions *VI* and *VII* in Fig. 2, the regions of weakly ionized and strongly ionized plasma.

The electrical conductivity of plasma in the region of intermediate degrees of ionization is calculated by the Chapman–Enskog method of successive approximations. This method converges poorly. As a result, a number of interpolation formulas have been suggested, such as that of Frost:

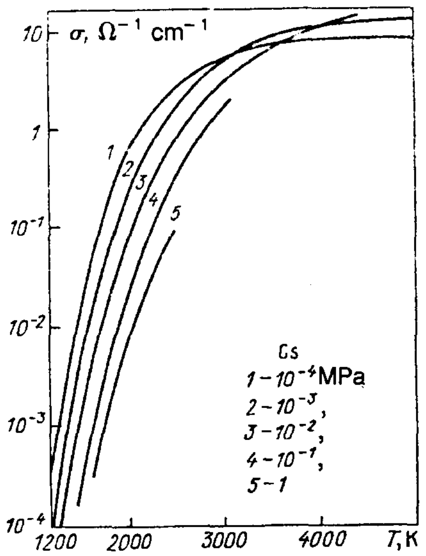

FIG. 3. Isobars of the electrical conductivity for a cesium plasma.[4]

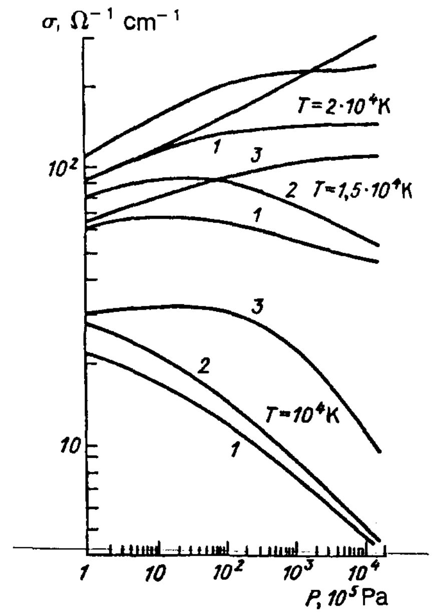

FIG. 4. Isotherms of the electrical conductivity for a partially ionized argon plasma.[5] *1*) Frost formula; *2*) Chapman–Enskog method; *3*) additive approximation.

$$\sigma=(4/3\sqrt{\pi})e^2N_em^{-1}T^{-5/2}\int_0^\infty E^{3/2}(\nu(E)+\nu_i(E)\gamma_E^{-1})e^{-E/T}\mathrm{d}E, \tag{8}$$

where $\nu_i(E)$ is the electron–ion collision frequency,

$$\nu_i(E)=2\pi Z^2e^4E^{-3/2}N_i(2m)^{-1/2}\ln\Lambda.$$

Figure 3 displays the calculated electrical conductivity of cesium as a function of temperature. At high temperatures all the $\sigma(T)$ curves approach the Spitzer values. They remain close together up to those temperatures at which the second ionization begins. At low temperatures, when the plasma is weakly ionized, the parameter $I/2T$ has the most effect on σ; it determines the electron density.

The range of pressures and temperatures in Fig. 3 is bounded by the conditions of weak coupling with respect to the Coulomb interaction, $\ln\Lambda\geqslant 3$, and with respect to ion–atomic interactions, $\Gamma_{ai}\leqslant 1$.

Figure 4 displays isotherms of the electrical conductivity of partially ionized argon plasma, calculated in various approximations.[5] The values given by Eq. (8) and obtained by solving the kinetic equation using the Chapman–Enskog method are very similar. The "additive" approximation, in which the separate resistances due to scattering by ions and atoms are added together, is quite crude.

The above formulas satisfactorily describe the experimental data. Figure 5 presents a comparison with recent results.[7] These experimental data apply to regions *VI* and *VII* in Fig. 2.

4. THE LIQUID METAL STATE

Another region in which the electrons can be regarded as almost free is that corresponding to liquid metals. Although the electron–electron coupling parameter $\Gamma_{ee}=r_s$ is close to unity and in some cases larger, as is well known, the approximation in which the electrons are regarded as almost free is quite satisfactory. However, the range of liquid metal states of interest to us includes the poorly studied vicinity of the melting point and the region of the so-called expanded liquid-metal states. The experimental data obtained in a number of laboratories indicate that the electrical conductivity decreases as the density decreases, with this behavior becoming quite marked as one approaches the critical point (Fig. 6).

This change in the electrical conductivity reflects the change of state in the electron subsystem, from almost free electrons to strongly interacting electrons (since r_s increases sharply) and to partially localized electrons. To what extent does the conventional theory of electrical con-

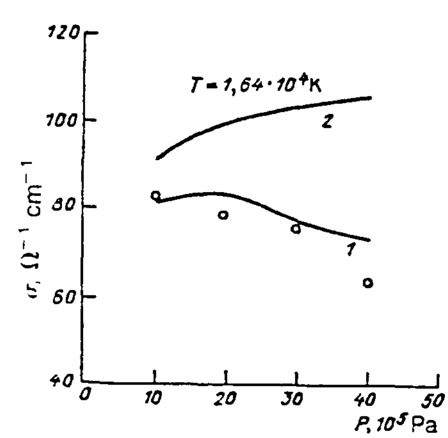

FIG. 5. Electrical conductivity of a weakly ionized argon plasma.[6] Calculated values are: *1*) Chapman–Enskog method; *2*) the points correspond to experiment.[7]

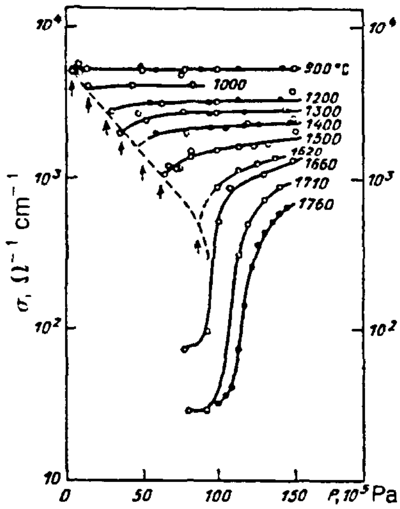

FIG. 6. Isotherms of the electrical conductivity for cesium in the liquid region and near the metal–insulator transition.[8]

ductivity in liquid metals remain valid for the broadened states?

This theory is based on the fact that almost free electrons experience excessive scattering events with highly correlated ions. The ions, even very far from degeneracy, interact strongly, $\Gamma_{ZZ} \gg 1$. This allows us to use the Lorentz gas approximation, but in averaging over the spatial distribution of the scatterers we must necessarily take into account their correlations. Consequently, the formula for σ contains an ion structure factor $S(q)$:

$$\sigma = E_F^{3/2}(2^{1/2}\pi Z e^2 m^{1/2})^{-1} \times \int_0^\infty E^3 (\ln \Lambda)^{-1}(-\mathrm{d}f/\mathrm{d}E)\mathrm{d}E, \tag{9}$$

$$\ln \Lambda = \int_0^{q_m} (V(q)/4\pi Z e^2)^2 S(q) q^3 \mathrm{d}q;$$

here $f = \{1+\exp[E-\mu)/T]\}^{-1}$ is the electron energy distribution function, and μ is the electron chemical potential, which is related to the electron density by

$$E_F^{3/2} = (2/3)\int_0^\infty E^{1/2} f(E)\mathrm{d}E,$$

where E_F is the Fermi energy, $q_m = 2(2mE)^{1/2}\hbar^{-1}$ is the maximum momentum transferred, and $V(q)$ is the Fourier component of the scattering potential. This last can be taken in various approximations: the Fourier component of the Coulomb potential or a pseudopotential, or it can be divided by the electron dielectric constant in order to take into account the coupling of the electron subsystem.

If the electrons are highly degenerate, the result is just the Ziman formula for the electrical conductivity of a liquid metal:

$$\sigma = E_F^{3/2}(\sqrt{2}\pi Z e^2 m^{1/2} \ln \Lambda)^{-1}, \quad \ln \Lambda = \int_0^{2k_F} (V(q)/4\pi Z e^2)^2 S(q) q^3 \mathrm{d}q, \tag{10}$$

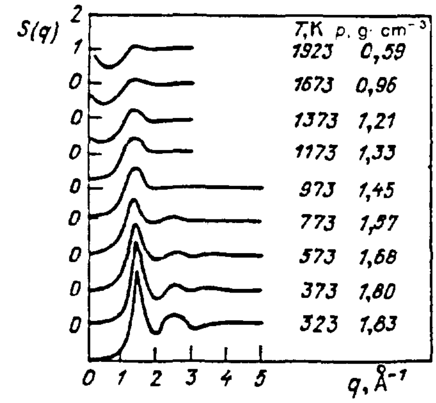

FIG. 7. Structure factor for cesium.[9]

where k_F is the Fermi momentum. This formula and more elaborate versions of it have been applied successfully to describe the electrical conductivity of liquid metals; see, e.g., Ref. 10.

The structure factor is the most important property of a dense medium. It is directly related to the binary correlation function $g(r)$ of the ions:

$$S(q) = 1 + N_i \int \exp(-\mathrm{i}qr)(g(r)-1)\mathrm{d}^3 r. \tag{11}$$

Exhaustive information about the structure factor of classical Coulomb systems has been obtained by modeling the thermodynamics of a one-component plasma (see, e.g., Ref. 1). The structure factor can be found in experiments on the scattering of neutrons or γ radiation. For expanded rubidium and cesium this has been done by Winter and Hensel.[9] Figure 7 displays the results of measurements of $S(q)$ carried out in liquid cesium from the melting point to the critical point. We see how gradually the close ordering disappears, which is clearly evident in the neighborhood of the melting point where $\Gamma_{ZZ} = 183$. Close to the critical point the medium is highly ordered. There the average coordination number drops from 8.5 to 2.7.

Redmer *et al.*[11] have compared the results calculated from the Ziman formula with experimental data obtained for highly expanded cesium (Fig. 8). Somewhere in the range of densities close to twice the critical values the theory systematically exaggerates σ. This is because the concept of free electrons is no longer applicable. This is plausible if we recall that near the critical point the metal–insulator transition occurs.

Note that Eq. (10) has another region where it cannot be applied. It is applicable for weakly coupled plasmas, i.e., those heated to the point where $\Gamma_{ZZ} < 1$ holds but with the electrons still degenerate. A formula for the electrical conductivity can be obtained with logarithmic accuracy by neglecting the ion–ion correlation in (10) and integrating from q_{min} to q_{max}. The result agrees in structure with the Spitzer formula if we replace the temperature there with the Fermi energy and the Debye screening radius with the Fermi radius.

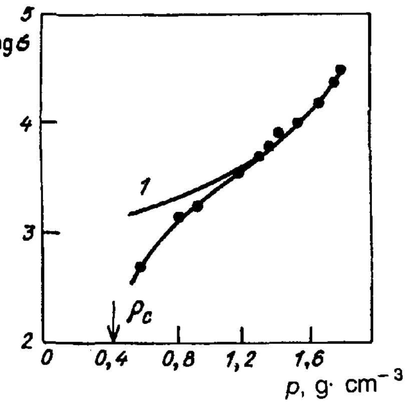

FIG. 8. Discrepancy between the measured values of the electrical conductivity of cesium near the critical point (points) and the results calculated from the Ziman formula (trace *1*).[11]

In a degenerate plasma no problem arises with electron–electron collisions. Their effect is suppressed by the Pauli principle.

5. ELECTRICAL CONDUCTIVITY NEAR THE CRITICAL POINT OF METALS

When the density is continuously reduced to the critical point and below a transition to the nonmetallic state and a sharp reduction in σ results (Fig. 9; region *II* in Fig. 2). This is the Mott transition. In systems that have been heated up it does not occur abruptly, but over a relatively broad range of densities. As is well known, the microscopic description of this transition is very complicated. A phenomenological theory is given below.[12,13] According to Likal'ner,[12] it is necessary to begin by noting that intermediate states exist between the metal state and the weakly ionized gas. In these the electrons cannot be regarded as either free or bound. One can take as the basic picture that of a gas of atoms in which the electron shells partly overlap in the ground state. We determine the radius of the shell as the radius of that of the classically allowed region of motion of the valence electrons; it is equal to e^2/I, where I is

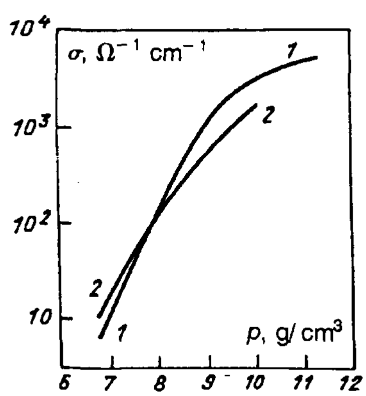

FIG. 9. Electrical conductivity of mercury as a function of density for $T=1800$ K. *1*) Theory (Ref. 12); *2*) experiment.[14]

the ionization energy of an atom. If these regions overlap, classical exchange by the electrons becomes possible.

The fraction of the plasma volume allowed for the valence electrons is consequently given by the expression

$$\xi_0=\mathcal{N}(4\pi/3)(e^2/I)^3N_i, \tag{12}$$

where $N_i=\rho/M$, and ρ is the material density. The fraction of allowed volume has two characteristic values. The value $\xi_0=0.29$ characterizes the so-called flow threshold. Only at $\xi_0=0.29$ does the "infinite cluster" develop. This is a connected allowed region penetrating the volume of the entire plasma. Electrons can propagate through this region, although they do not act completely free. The other characteristic value corresponds to dense packing of allowed regions of radius e^2/I, specifically $\xi_0=0.74$. For $\xi_0=0.74$ the whole plasma volume becomes classically accessible. Hence the electrons move as though they were free. The interval between 0.29 and 0.74 corresponds to the range of densities over which the Mott transition occurs. For the alkali metals this is the range of densities from half to twice the critical density. The electrical conductivity is determined by the formula

$$\sigma=eN_e\langle\mu_p\rangle, \tag{13}$$

where $\langle\mu_p\rangle$ is the mobility of an electron with momentum p, averaged over the momenta. An electron with energy $p^2/2m$ has an allowed region somewhat broader than ξ_0, specifically,

$$\xi_p=\xi_0[1-(p^2/2mI)^3]. \tag{14}$$

Below the flow threshold $\xi_0<0.29$ this mobility vanishes. For $\xi_p>0.74$ the mobility is equal to that of a free electron, μ_p. In Ref. 12 it was suggested that μ_p depends only on ξ_p and this dependence was approximated linearly within the specified interval of ξ_p.

After averaging the following approximate formulas are obtained. In the range $\xi_p<0.29$ the mobility falls off exponentially as the material is cooled,

$$\langle\mu_p/\mu_m\rangle=(2/\sqrt{\pi})\Delta_1(\Delta_2-\Delta_1)^{-1} \times(T/\Delta_1^{\frac{1}{2}}\exp(-\Delta_1/T), \quad \Delta_1\gg T.$$

For $0.29<\xi_0<0.74$ we find

$$\langle\mu_p\rangle/\mu_m=[(3T/2)-\Delta_1)](\Delta_2-\Delta_1)^{-1}, \quad \Delta_2\gg T;$$

here the energies Δ_1 and Δ_2 determine the flow energy level and the free propagation energy level for a given density:

$$\Delta_1=I[1-(\xi_0/0.29)^{1/3}],$$

$$\Delta_2=I[1-(\xi_0/0.74)^{1/3}].$$

On the high-density side the region where these expressions are applicable is bounded by the applicability of Boltzmann statistics. But in fact this is almost the entire region.

The theory provides a good description of the electron coefficients near the metal–insulator transition. Figure 9 displays a comparison for the electrical conductivity of mercury.

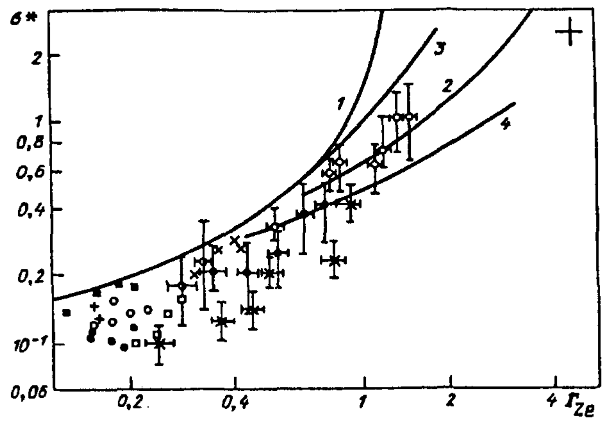

FIG. 10. Dimensionless electrical conductivity σ^* of a plasma as a function of the coupling parameter.[16] Theory: *1)* $\sigma^*_{\rm Sp}$; *2)* t-matrix approximation; *3)* Eq. (14); *4)* Eq. (15). Experiment: points correspond to the results of various authors (bibliography given in Ref. 16); the large straight cross shows the data of Ref. 17.

6. ELECTRICAL CONDUCTIVITY OF A STRONGLY COUPLED HIGHLY IONIZED PLASMA

The electrical conductivity of a strongly coupled highly ionized plasma has been measured in a considerable number of laboratories. Adequately uniform plasma regions were produced by heating and compressing material in shock waves, and also by pulsed ohmic heating. In the shock-wave experiments the strongest coupling, corresponding to $\Gamma_D=4$, was achieved by compressing xenon near the critical point behind a reflected shock wave.[15] This value of Γ_D corresponds to the Madelung strong coupling parameter $\Gamma_{Ze}=1.75$.

Figure 10 shows values of the dimensionless electrical conductivity as a function of the parameter Γ_{Ze}

$$\sigma^*=\sigma Ze^2m^{1/2}T^{-3/2}. \qquad (15)$$

The reduced conductivity σ^* is a universal property of the classical Coulomb system. In a strongly coupled plasma it is precisely this parameter Γ_{Ze} that characterizes the intensity of the electron–ion interaction, since the correlation radius becomes close to the average separation between ions. As for the Debye radius, it falls off and becomes smaller than $\bar{r}$, and so no longer characterizes the screening.

Large values of the coupling have been achieved by passing powerful current pulses through capillaries.[17,18] In Ref. 17 the electrical conductivity of a copper plasma was measured at densities 1–2 g/cm^3 and temperatures $(6\text{–}10)\cdot 10^3$ K. Figure 10 shows how these results are related to the others for $\Gamma_{Ze}\approx 5$. To reliably relate these values of the electrical conductivity to the thermodynamic parameters requires exercising a special hydrodynamic code in order to describe the plasma expansion and its reflection from the capillary walls.

Note that the plasma that arises in these experiments,[17] is already at the edge of degeneracy, since the temperature is close to the Fermi energy. The electron–ion interaction in a degenerate plasma is characterized by the parameter r_s. In the experiment of Ref. 17 this parameter has the very same value, close to 5.

These experimental data definitely imply that the values of the electrical conductivity are reduced in comparison with those given by the Spitzer formula. Asymptotic expressions which improve on the Spitzer formula by retaining the nonlogarithmic terms in the expansion of σ only increase this discrepancy. It is understandable that the Spitzer formula does not work here, since the basic assumptions of the kinetic theory are violated. What is more surprising is that it yields reasonable values up until Γ_{Ze} is close to unity.

The problem is how to derive new expressions for σ which go over to the correct limiting formulas and accurately describe the experimental data.

For this purpose Gryznov *et al.*[19] has suggested a model which approximately includes the increasing interparticle correlation. The starting point is expression (9), which treats the time-independent Debye shielding of the electron–ion potential and in the same approximation uses the structure factor

$$V(q)/4\pi Ze^2=(q^2+q_D^2),\quad S(q)=q^2(q^2+q_D^2)^{-1},$$

where $q_D=r_D^{-1}$. To reach the asymptotic Spitzer form for σ to within the electron–electron scattering terms, we must take the value of the maximum momentum that can be transferred equal to $2E/Ze^2$. This should not arouse any objections, since it is close to the inverse value of the Coulomb scattering amplitude.

For a nondegenerate plasma we find an expression for σ in which the place of the Coulomb logarithm is taken by a more complicated expression

$$\ln\Lambda=\tfrac{1}{2}[\ln(1+\alpha^2)-\alpha^2(1+\alpha^2)^{-1}-\tfrac{1}{2}\alpha^4(1+\alpha^2)^2],$$

where $\alpha=q_m r_D$. In the weak-coupling limit $\ln\Lambda=1$, this expression goes over to the usual Coulomb logarithm $\ln\Lambda=\ln(\alpha/2)$. In a strongly coupled plasma the expression for σ, in contrast to that of Spitzer, does not contain an unphysical divergence. In Fig. 10 trace *3* corresponds to

$$\sigma^*=2^{5/2}\pi^{-3/2}\gamma_E(\ln\Lambda)^{-1}.$$

The logarithm $\ln\Lambda$ is calculated according to (14).

Another simple model,[6] which also solves this problem, is related to the use of the so-called muffin-tin (MT) potential $V(r)=-Ze^2/r$ for $r\leqslant\bar{r}$ and $V(r)=0$ for $r>\bar{r}$ as the electron–ion potential.

The radius of the MT sphere is chosen equal to the average ion-ion separation. This choice correctly reflects the fact that in the strong coupling region it is $\bar{r}$ that becomes the screening radius. The electron–ion momentum-transfer cross section for scattering by the MT potential takes the form

$$q(E)=2\pi\bar{r}^2[\xi^2(\xi^2-1)^2\ln\xi^2-(\xi^2-1)],$$

$$\xi=2\bar{r}E/e^2.$$

In Ref. 6 we used this cross section to solve the kinetic equation by the Chapman–Enskog method. As a result of

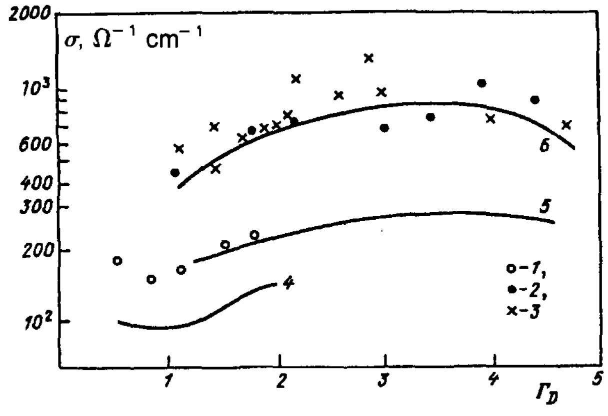

FIG. 11. Electrical conductivity of a strongly coupled plasma made up of argon and xenon. Experiment: *1*) argon;[21] *2*) xenon;[21] *3*) xenon.[15] Calculated values:[20] *4*) argon; *5*) xenon for conditions corresponding to Ref. 21; *6*) xenon under conditions corresponding to Ref. 15.

the calculations carried out for $0.5 < \Gamma_D < 10$, a simple approximation was proposed for the electrical conductivity of such a plasma:

$$\sigma^* = 0.591[1 + \delta(\Gamma_D - \Gamma_{D0})],$$

where $\delta = 0.155$, $\Gamma_{D0} = 3.6$. This is shown in Fig. 10. In particular, it was found that for a plasma with singly charged ions the factor that takes into account the electron–electron collision effects is $\gamma_E(1) = 0.71$.

A direct comparison with the values of σ for a partially ionized plasma, measured by Ivanov *et al.*,[21] which was carried out in Refs. 6 and 20, showed that the calculated values are substantially smaller than the measured ones (Fig. 11). It is unclear whether this represents shortcomings in the theory or errors in processing the directly measured quantities.

Let us now turn to work carried out using generalized kinetic equations. Ropke and Redmer[22] found an interpolation formula for the electrical conductivity of a nondegenerate plasma. It is valid provided that the parameters Γ_{Ze} and T/E_F have values of order unity. Ichimaru and Tanaka[23] obtained approximations which are valid for any degree of degeneracy.

Nevertheless, at large values of the coupling parameters the fundamental underlying assumptions of the kinetic theory become invalid. When we eliminate the problems with long-range collisions (using the Coulomb logarithm) we must keep in mind that even close encounters involve more than two particles at a time. The electron mean free path $[(Ze^2/T)^2 N_i]^{-1}$ becomes comparable with the scattering length Ze^2/T and with the average distance between scatterers $N_i^{-1/3}$. Under these conditions we need an alternative to the gas kinetic approximation. This may be supplied by the cellular model of a plasma.

7. ELECTRICAL CONDUCTIVITY OF A CELLULAR PLASMA

As the density increases the ion–ion interaction parameter $\Gamma_{ZZ} = Z^2e^2/\bar{r}T$ becomes large. The ions tend to move as far as possible from one another. Under these conditions the cellular approximation becomes applicable. The entire material is divided up into spherical cells of radius $\bar{r}$, each of which contains an ion screened by Z electrons. This physical picture is in complete agreement with the results of numerical simulation of the structure which have been carried out using the one-component model of a plasma by Hansen and his collaborators (see, e.g., Ref. 1). The simplest form of this model is that in which the electron–electron interaction can be ignored in a multiply ionized plasma, while the electron–ion interactions can be treated as weak, i.e., when the inequality (3) is satisfied. Then we can assume that the distribution of the free electrons in a cell is completely uniform. The electron–ion cellular potential is given by the solution of the Poisson–Boltzmann equation with the boundary conditions

$$V = -(Ze^2/\bar{r})\Phi(r/\bar{r}),$$
$$\Phi(x) = x^{-1}(1 - 3x/2 + x^3/2). \qquad (16)$$

This approximation turns out not to be too bad even for $\Gamma_{Ze} \approx 1$. In fact, even for $\Gamma_{Ze} \gg 1$ the equilibrium distribution of free electrons (those with total energy greater than zero) in this potential contains no large parameters:

$$N_e(r) \approx Z(4\pi\bar{r}^3/3)^{-1}A^{-1}\Phi(r/\bar{r})^{1/2},$$

$$A = 3\int_0^1 \Phi^{1/2}x^2 dx.$$

In the main part of the cellular volume the electrons are distributed almost uniformly.

The potential $V(r)$ has a short range, and the effective potential has a centrifugal barrier. The free electrons entering the cell with large impact parameters are reflected from the barrier without getting very far into the cell. However, for large values of Γ_{Ze} they represent a small fraction, corresponding to an impact parameter b such that

$$\bar{r}[1 - (3\Gamma_{Ze})^{-1}] < b \leqslant \bar{r};$$

here $\Gamma_{Ze} = 2Ze^2/\bar{r}mv^2$ is the interaction parameter for an electron with velocity v on entrance to the cell. The majority of the electrons are drawn into the cell and in circumventing the ion along a half circle with small radius they traverse a total path of length $2\bar{r}$. If we divide this by the average velocity v_{av}, we find that the time required to cross the cell is $2\bar{r}/v_{av}$.

We can write the average electron velocity approximately in the form $v_{av} = v_{T(F)}(1 + \Gamma_{Ze}^{1/2})$, where $v_{T(F)}$ is the electron thermal (or Fermi) velocity. Then we find for the electrical conductivity

$$\sigma = N_e e^2 \tau/m = (N_e e^2/m)\cdot 2\bar{r}v_{T(F)}^{-1}(1 + \Gamma_{Ze}^{1/2})^{-1}. \qquad (17)$$

For large Γ_{Ze} we find $\sigma \sim \omega_{pe}$, i.e., it is proportional to the electron plasma frequency $\omega_{pe} = (4\pi e^2 N_e/m)^{1/2}$. In the limit of large Γ_{Ze} the electrical conductivity must be proportional to ω_{pe} from dimensional considerations.

The assumption that the electrical conductivity is proportional to the plasma frequency was made by Kurilenkov and Valuev,[24] who argued from different physical considerations. According to them the electron dynamics is determined by scattering from thermal plasma oscillations. They assumed[24] that this mechanism is important even under conditions of moderate coupling, corresponding to those in the experiments of Fig. 10. Since that time the question about the role of scattering by plasma oscillations has remained unclear, although it has been discussed in the literature.

Equation (17) is a special case of the Ioffe–Regel' formula. In the gas kinetic approximation the electrical conductivity is proportional to the mean free path. It falls off as a function of the density. Ioffe and Regel' argued that there is a natural limit to the decrease in the mean free path. It cannot become smaller than the separation between the scatterers. But if the separation becomes smaller than the electron de Broglie wavelength λ, then the mean free path cannot be less than λ. The Ioffe–Regel' formula takes the form

$$\sigma=(\mathcal{N}_e^2/m)l_{\min}/v_{\mathrm{av}}, \tag{18}$$

where $l_{\min}$ is the shortest mean free path in the medium and v_{av} is its average velocity. The Ioffe–Regel' formula is said to determine the minimum electrical conductivity of a dense medium in which the density of the free electrons is given.

Let us pause briefly to discuss an important point. The domain of applicability of the cellular approximation allows high densities and temperatures to be treated. This is very important for the area of applications. These states occur when high-power energy pulses act on structural materials. At high temperatures an electron interacting with an ion which is not completely stripped can penetrate into its electron shells. The cellular potential now is characterized by at least three parameters Z_n, Z, and $\bar{r}$, where Z_n is the charge of the nucleus. A number of different approximations to $V(r)$ are possible. For example, in analogy with zinc[25] we can assume

$$V(r)=-(Z_n-Z)e^2r^{-1}(1+rR_c^{-1})^{-2}$$
$$\times(1-r/\bar{r})^{-1})+Ze^2\bar{r}^{-1}\Phi(r/\bar{r});$$

here $R_c=a_0(1.66Z^{1/3})^{-1}$ is the Thomas–Fermi radius of the ionic core and $\Phi(r/\bar{r})$ is given by the earlier expression (16). Including the ionic core enhances the interaction, effectively increasing the interaction parameter Γ_{Ze}.

8. WEAKLY COUPLED METAL VAPOR PLASMA; CLUSTER IONS

In a weakly ionized plasma the electrical conductivity is determined not so much by the electron mobility as by the degree of ionization. The latter in turn is determined by the parameter $I/2T$ (where I is the ionization energy), which appears in the argument of the exponential in the Saha equation which determines the degree of ionization. Hence the discussion of the ionization equilibrium becomes of primary importance. It is influenced mainly by the interaction between charged and neutral particles. In metal vapors this interaction, which is characterized by the parameter Γ_{ai} given by Eq. (4) becomes strong even for moderate densities due to the large values of the polarizability of metal atoms. It is manifested in the appearance and composition of the cluster ion plasma and as it turns out, at least in lowering the ionization potential.[1]

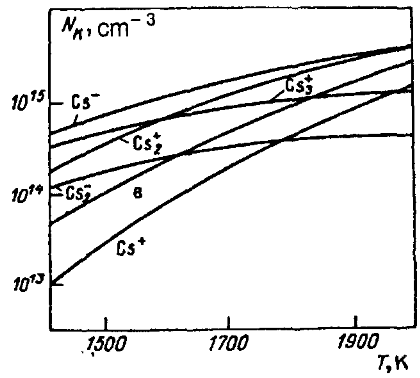

FIG. 12. Charged-particle density in a cesium vapor plasma on the $p=20$ atm isobar.[27]

At the present time quite a large volume of information has been gathered about heavy ion clusters.[26] In order to determine the composition of a plasma made up of electrons (e), atoms (A), diatomic molecules (A_2), di- and triatomic positively charged ions (A_2^+, A_3^+), and diatomic negatively charged ions (A_2^-) we consider the following equilibria:

$$\begin{aligned}
&e+A^+ \rightleftarrows A, && N_eN^+/N=K_1,\\
&e+A \rightleftarrows A^-, && N_eN/N^-=K_2,\\
&A+A \rightleftarrows A_2, && NN/N_2=K_3,\\
&A+A^+ \rightleftarrows A_2^+, && NN^+/N_2^+=K_4,\\
&A_2+A^+ \rightleftarrows A_3^+, && N_2N^+/N_3^+=K_5,\\
&e+A_2 \rightleftarrows A_2^-, && N_eN_2/N_2^-=K_6;
\end{aligned} \tag{19}$$

here K_i are the chemical equilibrium constants. Equation (19) together with the conditions for conservation of energy and total particle number yields

$$N_e^2=K_1N[(1+(N/K_4)+(N^2/K_3K_5)]$$
$$\times[(1+(N/K_2)+(N^2/K_3K_6)]^{-1}. \tag{20}$$

It is easy to see that the largest fraction in (20) reflects the effect of molecular modes on N_e. The individual terms in the numerator (denominator) of the fraction correspond to the composition of the various positive (negative) ions. It is obvious that including A_4^+ cluster ions would introduce another term in the denominator, etc.

Figure 12 displays the composition of the charged components of the plasma of a cesium vapor temperature, calculated on the $p=20$ atm isobar. It can be seen that as the temperature decreases the heavy ions play an increasingly important role. The A^+ ion, which dominates among the positive ions for $T>2200$ K, is replaced by the A_2^+ ion, which in turn replaces the A_3^+ ion. Hence we can expect that further cooling will cause heavier and heavier positive ions to form. Among the negatively charged components for $T<2000$ K the A^- ion dominates. However, the A_2^- ion remains insignificant and there is no reason to expect that significant concentrations of the A_3^- ion will appear as a result of further cooling. This behavior becomes more prominent as the coupling constant is made stronger.

Its symmetry is quite typical. It reflects the general pattern: the ion–atom or ion–molecule interaction is stronger than the electron–atom (or electron–molecule) interaction. The quantum nature of the electron is manifested in the fact that the binding energy of the negative complexes is smaller than the binding energy of the positive complexes. For example, the binding energy of Na_2^+ is equal to 1.02 eV, although the binding energy of Na^- is only 0.548 eV. At subcritical temperatures this difference is important. The dominance of the ion–atom interaction raises the electrical conductivity. This parameter region is labeled with *VI* in Fig. 2.

If we substitute the expression (20) for N_e obtained by including cluster ions in the expression for σ, then we can observe how the appearance of cluster ions alters the density dependence of σ. At large values of T and small values of N_a the relation $N_e \sim N_a^{1/2}$ holds in accordance with the Saha formula; the electrical conductivity decreases with density, $\sigma \sim N_a^{-1/2}$. When T decreases and N_a increases, cluster ions appear. If A_3^+ dominates among the positive ions and A^- dominates among the negative ones, then it is found that σ is independent of N_a. If the A_4^+ ion dominated, then σ would increase as a function of density, $\sigma \sim N_a^{1/2}$. In this section we restrict ourselves to the conditions such that the coupling parameter due to the ion–atom interaction satisfies $\Gamma_{ai}<1$.

Since this interaction can give rise to strong atom–ion correlations, as we see, then in contrast to the definition (4) the ion–atom interaction parameter in region *VI* is more correctly introduced as follows:

$$\Gamma = N_3^+/N_2^+ = NK_4/K_3K_5.$$

The condition $\Gamma_{ai}=1$ determines the boundary between regions *IV* and *VI* in Fig. 2. If $\Gamma_{ai}>1$ holds then $N_3^+>N_2^+$. This implies that we can anticipate that heavier ions will appear. Hence the range of parameters included by the calculations for the alkali metals,[4] is bounded by $\Gamma_{ai}<1$ (see Fig. 3). The results of these calculations agree fairly well with the available experimental data. In cesium vapor this region corresponds to $p<1$ atm and to temperatures of up to 2000 K.

The introduction of cluster ions determines the contribution of the interaction to the discrete spectrum. After the cluster ions form a residual interaction occurs in the continuous spectrum. Its result may be interpreted as a lowering of the ionization potential by ΔI, calculated by Likal'ter:

$$\Delta I = 1.61 \cdot 4\pi N_a T(\alpha e^2/2T)^{3/4}.$$

In moderately dense vapors ΔI is small and only at high densities does it begin to exceed the temperature.

The electron mobility in a medium of heavy uncorrelated scatterers is given by the Lorentz formula, which is valid when the interaction radius is much smaller than the electron mean free path. For this to hold the interaction sphere must contain less than two electrons, i.e., the inequality

$$(4\pi/3)N_a q^{3/2} \ll 1.$$

must hold. At densities $N_a=10^{20}$ cm^{-3} the quantity $(4\pi/3)N_a q^{3/2}$ in a cesium plasma reaches a value close to unity, since we have $q \approx 400\pi a_0^2$. This does not mean, however, that as the density increases the electron mobility μ becomes less than the mobility μ_0 calculated for the same density using the Lorentz formula. The electron–atom interaction cannot always be described by representing it in terms of a hard sphere of radius $q^{1/2}$. The electron–atom interaction occurs mainly through polarization, but overlapping of the "tails" of the interaction potentials can smear the potential field as a whole. As a result the mobility increases; this is well known in the physics of electronic phenomena in a number of liquids. Other density effects which play a part in the mobility are also well known.[28]

9. DROPLET MODEL OF A STRONGLY COUPLED METAL-VAPOR PLASMA

Metal vapors at and near the saturation line assume the form of a strongly coupled plasma (region *IV* in Fig. 2). Away from the immediate vicinity of the critical point this plasma can be regarded as weakly ionized. The main reason for the strong coupling in this case is the strong interaction between the charged and neutral particles. This interaction facilitates the formation of heavy charged clusters in the plasma. Their density increases as one approaches the saturation line. Then the density of positively charged clusters is substantially greater than the density of negative clusters. The electrical neutrality of the plasma gives rise to a corresponding increase in the electron density. This leads to an anomalously high conductivity for the vapor on the saturation line. Thus, the Saha and Lorentz formulas yield a value $\sigma = 5 \cdot 10^{-4}$ $(\Omega \cdot \mathrm{cm})^{-1}$ for the electrical conductivity of cesium at $T=1500$ K. The experimental value is $\sigma = 1$ $(\Omega \cdot \mathrm{cm})^{-1}$. On the vapor saturation curve the electrical conductivity is three orders of magnitude greater than the result of this estimate, carried out in the usual way for an ideal plasma. When the heating takes place along an isobar the electrical conductivity first falls to a minimum value somewhat greater than that of an ideal plasma (see Fig. 1). Then it increases, approaching the perfect gas values.

In this range of temperatures and pressures uniform volumes of plasma can be obtained in resistive furnaces and the parameters can be determined with relatively high precision. Such measurements were carried out in the 1970s by Alekseev and Hensel. They demonstrated anomalously high electrical conductivity for saturated vapor and found a qualitatively new dependence on the isobars. Recent measurements by Hensel *et al.*[29] show that the effects found at that time were exaggerated. The quantities found now match well with the results of measurements carried out near saturation at temperatures of about 1200 K (Ref. 30; see Fig. 13).

It has been suggested[1] that the clusters that form near the saturation lines be regarded as liquid metal droplets. This permits the properties of the clusters to be determined by well known characteristics of metals, the surface tension and work function for electrons. If a heavy ion consists of a droplet of radius R, then the work function $W(R)$ for an electron to escape from it is related to the work function W from a planar surface by the familiar expression

$$W(R)=W\pm Ze^2/R^{-1},$$

Here the plus sign applies to positively charged ions and the minus sign to negatively charged ions. This asymmetry is the same as that discussed in the previous section. For cluster dimensions typical of plasmas, the difference in binding energies between positive and negative clusters is so large that the negatively charged clusters can be neglected in general. We will assume that the plasma consists of atoms, positively charged droplets, and electrons. The particle densities are N_a, N^+, and N_e and the total number of all particles is $\tilde{N}=N_a+N^++N_e$. The thermodynamic potential of this system takes the form

$$\Phi=N_a\varphi_a+N^+[g\varphi_L+4\pi\gamma R^2+W+(e^2/2R)] + \sum_k N_k\ln(N_k/\tilde{N}); \tag{21}$$

here φ_L and φ_a are the thermodynamic potentials of the liquid and vapor for a single atom, so that the quantity

$$gT\ln p_s/p=g(\varphi_L-\varphi_a),$$

is the energy of formation of a neutral droplet of radius R,

$$g=(4\pi/3)R^3N_L$$

is the number of particles in a droplet, N_L is the particle density in the liquid, p_s is the saturation pressure, and $4\pi\gamma R^2$ is the surface energy of a droplet. In the final entropic term in Eq. (21) the summation is carried out over all species of particles. This simple approach enables us to get away with using a qualitative description of the effect. From (21) the following results are obtained. In the saturated vapor the radius of the most probable droplet is equal to the "electrocapillary" radius $R=(e^2/16\pi\gamma)^{1/3}$. At the pressure 40.3 atm of saturated cesium vapor, which corresponds to $T=1600$ K, such a droplet consists of twenty cesium atoms. These droplets are of course too small for a macroscopic description to be completely correct. However, in the theory of nucleation it is usually assumed that droplets containing more than ten particles are macroscopic. Such droplets are treated in descriptions of the heterogeneous nucleation in saturated vapor.

From (21) the ionization equilibrium equation then follows:

$$N_e=N\exp\left[-(W+4\pi\gamma R^2+e^2R^{-1})\cdot\frac{1}{2T}\right] =N\exp\left[-\left(W+\frac{3e^2}{4R}\right)\cdot\frac{1}{2T}\right]. \tag{22}$$

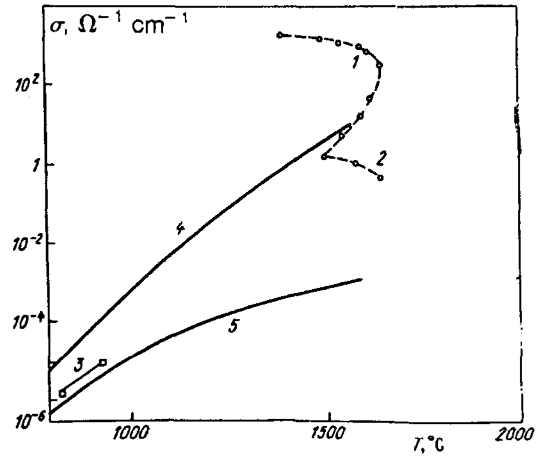

FIG. 13. Electrical conductivity of a dense cesium vapor. Experiment: *1*) on the phase coexistence curve;[29] *2*) on the 65-atm isobar;[29] *3*) in vapor near saturation.[30] The theory for saturated vapor is *4*) droplet model,[34] *5*) ideal gas approximation.

For a number of reasons the coefficient multiplying the exponential in Eq. (22) is known very poorly. Consequently, we discuss the exponential which is what is responsible for the main effect. The argument of the exponential contains W, the work function of an electron escaping from metal, which is well known to decrease as a function of the metal temperature (as the density decreases), vanishing at the critical point. For example,

$$W(T)=W_m(T_c-T)(T_c-T_m)^{-1},$$

where T_c and T_m are the critical temperature and the temperature at the melting point, in which the value of the work function W_m is taken to be 1.8 eV for cesium.

The results of the calculations show that the electron densities are very large. The interaction effects lead to enhancement of N_e by orders of magnitude relative to the perfect-gas approximation. However, this simple analysis is too crude. In a number of treatments the droplet model has been substantially improved. Figure 13 compares the values of the electrical conductivity for cesium vapor near saturation with those calculated using the theory of Ref. 31. The theory describes the anomalous electrical conductivity and the transition to the normal conductivity which occurs as the pressure is reduced.

10. CALCULATIONS OF THE ELECTRICAL CONDUCTIVITY OVER A BROAD RANGE

Applications have made it necessary to carry out calculations over a broad range. An example is the study of the behavior of structural materials subjected to high-power pulses of energetic radiation. With high energy inputs the material can pass through a considerable range of states as it heats up and cools down: from gaseous densities to solid densities, from temperatures on the order of standard temperature to hundreds of eV. Let us discuss the formulation and results of some calculations carried out over wide ranges.

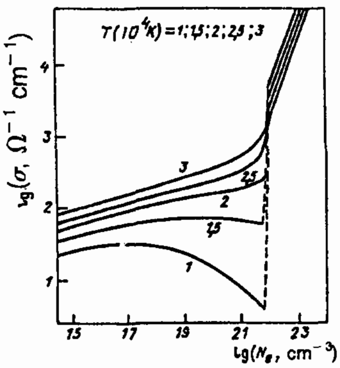

FIG. 14. Electrical conductivity of a hydrogen plasma as a function of N_e for various temperatures T (in units of 10^4 K) (Ref. 32). The broken line shows the Mott transition.

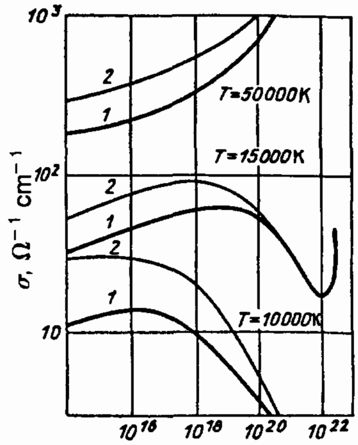

FIG. 15. Electrical conductivity of a hydrogen plasma calculated including (*1*) and excluding (*2*) for electron–electron interactions.[33]

One of the most systematic approaches is based on the Green's function method, used to write down the kinetic equation in which the collision integral is represented in the form of a combination of unshielded t-matrix collision integrals, an unshielded Born integral, and a Born integral with dynamic shielding. Furthermore, the electron–atom collisions must be taken into account (in order to describe partial ionization) along with electron–electron interactions. The result of such a treatment would go over satisfactorily to the exact limiting expressions. Results of a broad range of studies have been presented[6] which clarify the effect of the various physical factors on the electrical conductivity.

We present some results. Figure 14 shows the electrical conductivity as a function of electron temperature and density. The conductivity was calculated in the second Born approximation with dynamic shielding. The role of the minimum impact parameter is played by the thermal wavelength and the Landau length. At low and high densities σ has the Lorentz and Ziman asymptotic forms. The equation for ionization equilibrium, whose solution yields the electron density, describes both the thermal ionization and the ionization associated with high compression. The broken trace in Fig. 14 corresponds to the Mott transition, which in this approximation is a discontinuity rather than continuous. The minimum values of the electrical conductivity in Fig. 14 are determined by electrons scattering from atoms. At densities above the Mott transition the electrical conductivity is given by the Ziman formula.

The role of electron–electron interactions is largest at low charged-particle densities, when it is given by the Spitzer factor γ_E. It decreases with increasing coupling constant and finally vanishes for highly degenerate materials under the influence of the Pauli principle[33] (Fig. 15).

In Fig. 10 the results of the calculations are compared with the experimental results discussed in one of the previous sections of the present review.

In another series of papers (Refs. 23, 34; reviewed in Ref. 35) the theory of two-particle correlations is reworked using the dielectric-function formalism in the theory of a linear response. These results constitute a generalization of the Ziman formula to finite temperatures. The electron–ion potential is taken to be given by the Born approximation with dynamic shielding. For a fully ionized hydrogen plasma the Coulomb logarithm ln Λ has been tabulated, using the following expression:

$$\sigma^{-1}=4\cdot(2\pi/3)\Gamma^{2/3}\omega_{pe}^{-1}\ln\Lambda.$$

Tanaka *et al.*[34] has treated the enhancement of exchange and the correlations, extending the region of applicability of the theory to the region of the Mott transition. Figure 16 shows ln Λ for conditions such that $E_F=T$.

One of the most constructive and physically clear approaches was suggested by Lee and More for a dense hot plasma.[36] It is based on using the solution of the kinetic equation in the τ approximation, matching the expressions for the Coulomb logarithm that are valid in the various regions, and imposing additional physical assumptions. The whole temperature–density plane is broken up into several regions (Fig. 17). In the region *1*, where the plasma is weakly coupled, the Coulomb logarithm is calculated in the conventional manner:

$$\ln\Lambda=(1/2)\ln[1+(b_{max}/b_{min})^2],$$

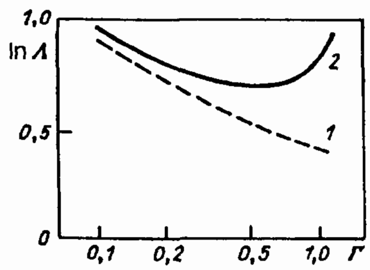

FIG. 16. Coulomb logarithm as a function of the strong coupling parameter, $T=E_F$. Trace *1* corresponds to Ref. 23 and trace *2* to Ref. 34.

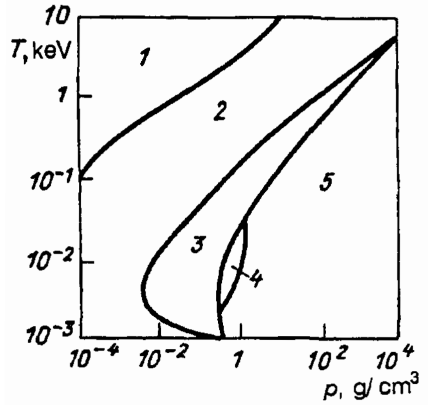

FIG. 17. Phase diagram in $\rho - T$ space for aluminum for analyzing the electrical conductivity.[36] *1*) Debye and Thomas–Fermi shielding; *2*) shielding at the average ion–ion separation; *3*) $\ln \Lambda = 2$; *4*) $\sigma = \sigma_{\min}$; *5*) Ziman region.

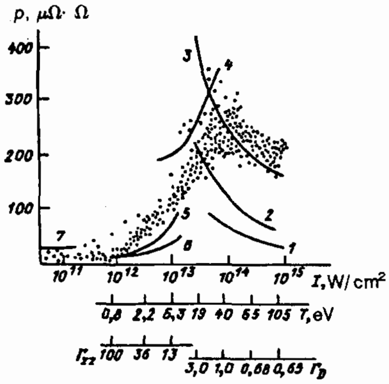

FIG. 18. Aluminum resistivity on the 2.7 g/cm³ isochore. *1*) Intensity of the heating radiation. The region of the points is the experiment of Ref. 38. Calculated:[39] *1*) Eq. (6); *2*) recalculation of the data according to σ^*; *3*) Eq. (23); *4*) Eq. (18); *5*) Eq. (10); *6*) Eq. (9); *7*) resistivity of liquid Al.

where $b_{\max}$ and $b_{\min}$ are the maximum and minimum impact parameters. As the shielding length $b_{\max}$ we use the Debye and Thomas–Fermi radii, while the minimum impact parameter is taken to be equal either to the Landau length or to the thermal wavelength. In the strongly coupled plasma region (region *2*), where the average interparticle separation becomes larger than the Debye length (the Fermi length), which is what is used for $b_{\max}$. If $\ln \Lambda$ is still found to be less than 2 it is taken equal to 2. This is region *3* in Fig. 17. In the region of the Mott transition σ is taken equal to the minimum Mott conductivity of the metal, while in a strongly correlated degenerate system for the electrical conductivity a Ziman expression is used. In this way constructive models are used, which enable us to find a universal estimate for σ.

The wide-range approach described in Ref. 37 has much in common with the model of Ref. 36, but the interpolation formulas are organized so that they embrace in a unified manner the entire range of parameters. In Ref. 37 the electrical conductivity of the metals Al, Fe, Cu, Au, Pb, Bi, and U was tabulated.

In connection with isochoric heating from the melting temperature to 100 eV the material passes through a whole series of strongly coupled plasma states, beginning with metallic and ending with gaseous. Milchberg and Freeman[38] constructed the 2.7 g/cm³ isochore for the resistivity of aluminum (Fig. 18) by processing the results of measuring the reflection coefficient for light coming from the surface of aluminum heated by a high-power laser pulse. The pulse length was so short (400 fs) that the medium was unable to expand during this time and retained its initial density. The temperature was measured simultaneously. On this isochore the ion charge was $Z=3$ up to 50 eV (the result of cold ionization, characteristic of the unheated specimen); thermal ionization yielded $Z=6$ at 105 eV. Yakubov[39] compared these values of the resistivity with those calculated over a wide range of conditions by the above methods.

The resistivity of a nondegenerate plasma ($T > E_F$) is not given by the Spitzer formula (trace *1* in Fig. 17) nor by the dimensionless conductivity σ^* of a Coulomb plasma, familiar from experiment (trace *2*). In the latter case the resistivity is calculated as follows:

$$\rho = \rho^* (\gamma_E(Z)/\gamma_E(1))^{-1} T^{-3/2} (Ze^2 m^{1/2});$$

here we have written $\rho^* = (\sigma^*)^{-1}$, and the values of σ^* are shown in Fig. 10. In describing the observed values of ρ it was found to be important to include scattering from the core of the complex Al^{+Z} ion. At high temperatures the amplitude $Ze^2/3T$ for Coulomb scattering is comparable with the radius R_i of the ion core. A rough estimate, taking into account the non-Coulomb component of the scattering, is made in the additive approximation (trace 3):

$$\rho = \rho_c + \rho_{nc},$$

$$\rho_{nc}^{-1} = (N_e e/m)[(1+\Phi)\pi R_c^2 N_i v_T]^{-1}; \qquad (23)$$

here ρ_c and ρ_{nc} are the Coulomb and non-Coulomb components of the resistivity and Φ is the reduced potential of the ion core,

$$\Phi = Ze^2/R_i T.$$

It takes into account the effect of curvature of the electron orbits in the ion field on the Coulomb component. The value of R_i is taken to be $1.1 a_0$.

The calculated values must not exceed those given by the Ioffe–Regel' formula (18). The latter corresponds to trace *4*. In a degenerate plasma the calculation is performed using the Ziman formula (10), the Ashcroft pseudopotential, the Lindhardt dielectric function, and the structure factor for a one-component plasma. Here the choice of the radius of the pseudopotential is very problematical. Trace *5* indicates the increasing behavior of the electrical conductivity associated with heating. However, the measured temperature is that of the electrons. The ions are not able to heat up to this temperature. Trace *6* was obtained using Eq. (9) under the assumption that the ions heat up only to $T=0.8$ eV. Hence the degree of electron degeneracy was not restricted.

This comparison underscores the question about scattering from complex ions, although in general it confirms the validity of the calculation techniques used.

11. CONCLUSION

As is evident, despite significant successes we are still far from a satisfactory solution of the problem of the electrical conductivity of material over a broad range of densities and temperatures. Naturally, the situation varies depending on which part of the phase diagram we are considering.

In the regions where the plasma is strongly or moderately coupled we are concerned with errors in the calculated and experimental values of order tens of percent. The error in the calculated values is determined by the error in the initial data: the cross sections and scattering lengths and the parameters of the cluster ions.

In the strong-coupling region the values of the electrical conductivity can be estimated only in order of magnitude. Here the electron scattering mechanisms or mechanisms for ionization itself are sometimes controversial; in any case, the methods for describing them are. At any event, I hope that the qualitative picture of the behavior is correct. This is a big achievement. The quantitative changes may be wholesale.

This concerns most of all the conditions of very high compression, up to densities far in excess of normal. In this region it is especially necessary to obtain experimental data, although it is readily understood that a superdense plasma is difficult to produce and diagnose. Both questions of ionization equilibrium and questions of electron mobility are far from a satisfactory solution. Here it is worthwhile to point out questions about the ion charge distribution, how conductivity electrons are distinguished from the rest, how the mobilities vary with energy, the contribution of weakly coupled electrons to the electrical conductivity, scattering from the non-Coulomb potentials of complex ions, and also a number of other complicated questions. They have not been addressed in this review, since its purpose was to present those topics which are relatively clear.

APPENDIX: THE THERMOELECTRIC COEFFICIENT

In the presence of a temperature gradient Ohm's law acquired the form

$$\mathbf{F}+e^{-1}\nabla\mu=\sigma^{-1}\mathbf{j}+S\nabla T.$$

The left part contains the electric field strength F and the gradient of the electron chemical potential μ. In the right-hand side appears the thermoelectric coefficient (the thermal emf) S, which is closely related to the electrical conductivity. In Fig. 19 the isobars of the thermal emf are shown for cesium.[40]

For $T>3000$ K the plasma is ideal and can be obtained from the Lorentz gas approximation[3]

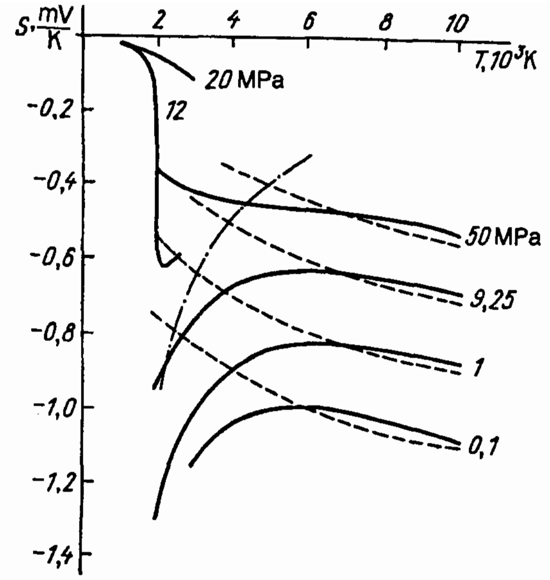

FIG. 19. Isobars of the thermal emf for cesium.[42] The calculated isobars 0.1, 1, 9.25, and 50 MPa are shown by solid traces. Their asymptotic limits given by Eq. (A2) and (A3) are shown by dashes and by chain curves. Results of the measurements[41,42] are the 12 and 20 MPa isobars.

$$S=(eT)^{-1}\left[\mu-\int_0^\infty E^2 f(E)\nu(E)^{-1}\mathrm{d}E\right.$$
$$\left.\times\left(\int_0^\infty Ef(E)\nu(E)^{-1}\mathrm{d}E\right)^{-1}\right], \qquad \text{(A1)}$$

where $\nu(E)$ is the collision frequency and $f(E)$ is the electron distribution function in energy E. For a highly ionized nondegenerate plasma (A1) yields

$$S=(eT)^{-1}(\mu+4T), \qquad \text{(A2)}$$

which depends weakly on T (dotted curves in Fig. 19). For small values of Z we need a factor here analogous to $\gamma_E(Z)$ in (2).

In a weakly ionized plasma when $I \gg T$ holds, the thermal emf is determined primarily from the ionization as a function of temperature. Since $\mu\approx T\ln(N_e\lambda^3)$, we have

$$S\approx -I(2eT)^{-1}. \qquad \text{(A3)}$$

It is easy to see that between S and σ there is a relation

$$S\approx-(T/e)\mathrm{d}\ln\sigma/\mathrm{d}T. \qquad \text{(A4)}$$

This expression is analogous to the Ziman relation for liquid metals,

$$S=-(pi^2T/3e)\mathrm{d}\ln\sigma/\mathrm{d}E_F. \qquad \text{(A5)}$$

In order of magnitude we have $S\approx -I(eE_F)^{-1}$.

The transition from an ideal plasma to the metal state is characterized by sharp changes in S, analogous to those that occur with the electrical conductivity; see, e.g., the form of the 12 MPa isobar in Fig. 18.

Probably behavior of the form shown in Fig. 19 is typical of simple metals. The thermal emf of such a "poor" metal as mercury changes sign not too far from the critical point.[43] The reason for this is unclear.

[1] V. E. Fortov and I. T. Iakubov, *Physics of Nonideal Plasma*, Hemisphere, New York (1989).

[2] V. A. Alekseev and I. T. Iakubov, in *Handbook of Thermodynamics and Transport Properties of Alkali Metals*, R. W. Ohse (ed.), Blackwell, Oxford (1985).

[3] E. M. Lifshitz and L. P. Pitaevskii, *Physical Kinetics*, Pergamon Press, Oxford (1981).

[4] V. V. Gogoleva, V. Yu. Zitserman, A. Ya. Polishchuk, and I. T. Yakubov, Teplofiz. Vys. Temp. **22**, 208 (1984).

[5] I. A. Mulenko and A. L. Khomkin, Teplofiz. Vys. Temp. **29**, 1234 (1991).

[6] I. A. Mulenko and A. L. Khomkin, IVTAN Preprint No. 1-326, Moscow (1991).

[7] M. M. Popovic, Yu. Vitel, and A. A. Minaylov, Invited Papers, Strongly Coupled Plasma, Yamanaka Lake (1989).

[8] F. Noll, W. C. Pilgrim, and R. Winter, Zs. Phys. Chemie **156**, 303 (1988).

[9] R. Winter and F. Hensel, Phys. Chem. Liq. **20**, 1 (1989).

[10] N. P. Kovalenko, Yu. P. Krasnyi, and S. A. Trizer, *Statistical Theory of Liquid Metals* [in Russian], Nauka, Moscow (1990).

[11] R. Redmer, H. Reinholz, and E. Noll, in 20th Intern. Conf. on Phenom. Ionized Gases, Contributed Papers, Vol. 1, Pisa (1991).

[12] A. A. Likal'ter, Teplofiz. Vys. Temp. **22**, 258 (1984).

[13] A. A. Likal'ter, Usp. Fiz. Nauk **162**, 119 (1992) [Sov. Phys. Usp. **35**, 591 (1992)].

[14] G. Schonherr, R. W. Schmutzler, and F. Hensel, Phil. Mag. **40B**, 411 (1979).

[15] V. B. Mintsev, V. K. Gryaznov, and V. E. Fortov, Zh. Éksp. Teor. Fiz. **79**, 116 (1980) [Sov. Phys. JETP **52**, 59 (1980)].

[16] W. D. Kraeft, D. Kremp, W. Ebeling, and G. Ropke, *Quantum Statistics of Charged Particle Systems*, Plenum, New York (1986).

[17] A. W. DeSilva and H.-J. Kunze, in *Physics of Nonideal Plasmas*, W. Ebeling, A. Forster, and R. Radtke (eds.), Teubner, Stuttgart–Leipzig (1992).

[18] J. F. Benage, L. A. Jones, R. L. Shepherd *et al.*, in *Strongly Coupled Plasma Physics*, S. Ichimaru (ed.), Elsevier, New York (1990).

[19] V. K. Gryaznov, Yu. V. Ivanov, A. N. Starostin, and V. E. Fortov, Teplofiz. Vys. Temp. **14**, 643 (1976).

[20] L. I. Podlubnyi, V. S. Rostovskii, and V. S. Filinov, Teplofiz. Vys. Temp. **26**, 218 (1988).

[21] Yu. V. Ivanov, V. B. Mintsev, V. E. Fortov, and A. N. Dremin, Zh. Éksp. Teor. Fiz. **71**, 216 (1976) [Sov. Phys. JETP **44**, 112 (1976)].

[22] G. Ropke and R. Redmer, Phys. Rev. **39A**, 907 (1989).

[23] S. Ichimaru and S. Tanaka, Phys. Rev. **32A**, 1790 (1985).

[24] Yu. K. Kurilenkov and A. A. Valuev, Beitr. Plasmaphys. **24**, 161 (1984).

[25] J. W. Zink, Phys. Rev. **176**, 179 (1968).

[26] B. M. Smirnov, *Cluster Ions* [in Russian], Nauka, Moscow (1983).

[27] A. G. Khrapak, Teplofiz. Vys. Temp. **17**, 1147 (1979).

[28] A. G. Khrapak and I. T. Yakubov, *Electrons in Dense Gases and Plasmas* [in Russian], Nauka, Moscow (1981).

[29] F. Hensel, M. Stolz, G. Nohl, R. Winter, and W. Gotzlaff, J. de Phys. IV **1**, C5-191 (1991).

[30] A. A. Borzhievskii, V. A. Sechenov, and V. I. Khorunzhenko, Teplofiz. Vys. Temp. **26**, 722 (1988).

[31] D. I. Zhukhovitskii, Teplofiz. Vys. Temp. **31**, 137 (1993).

[32] F. E. Hohne, R. Redmer, and H. Wegener, Physica **128A**, 643 (1984).

[33] M. Schlanges, D. Kremp, and H. Keuer, Ann. d. Phys. **41**, 54 (1984).

[34] S. Tanaka, X.-Z. Yan, and S. Ichimaru, Phys. Rev. **41A**, 5616 (1990).

[35] S. Ichimaru, H. Iyetomi, and S. Tanaka, Phys. Rep. **149**, 91 (1987).

[36] Y. T. Lee and R. M. More, Phys. Fluids **27**, 1273 (1984).

[37] W. Ebeling, A. Forster, V. E. Fortov, V. K. Gryaznov, and A. Ya. Polishchuk, *Thermophysical Properties of Hot Dense Plasmas*, Teubner, Stuttgart–Leipzig (1991).

[38] H. M. Milchberg and R. R. Freeman, Phys. Fluids **2B**, 1395 (1990).

[39] I. T. Yakubov, Teplofiz. Vys. Temp. **29**, 1028 (1991).

[40] H. Reinholz, R. Redmer, and G. Ropke, in 20th Intern. Conf. on Phenom. Ionized Gases, Contributed Papers, Vol. 4, Pisa (1991).

[41] V. A. Alekseev *et al.*, *High Temp.-High Press.* 7, 677 (1975).

[42] H. P. Pfeiffer, W. Freyland, and F. Hensel, Phys. Lett. **73A**, 111 (1973).

[43] W. Gotzlaff, Thesis, Marburg Univ. (1988).

Translated by D. L. Book